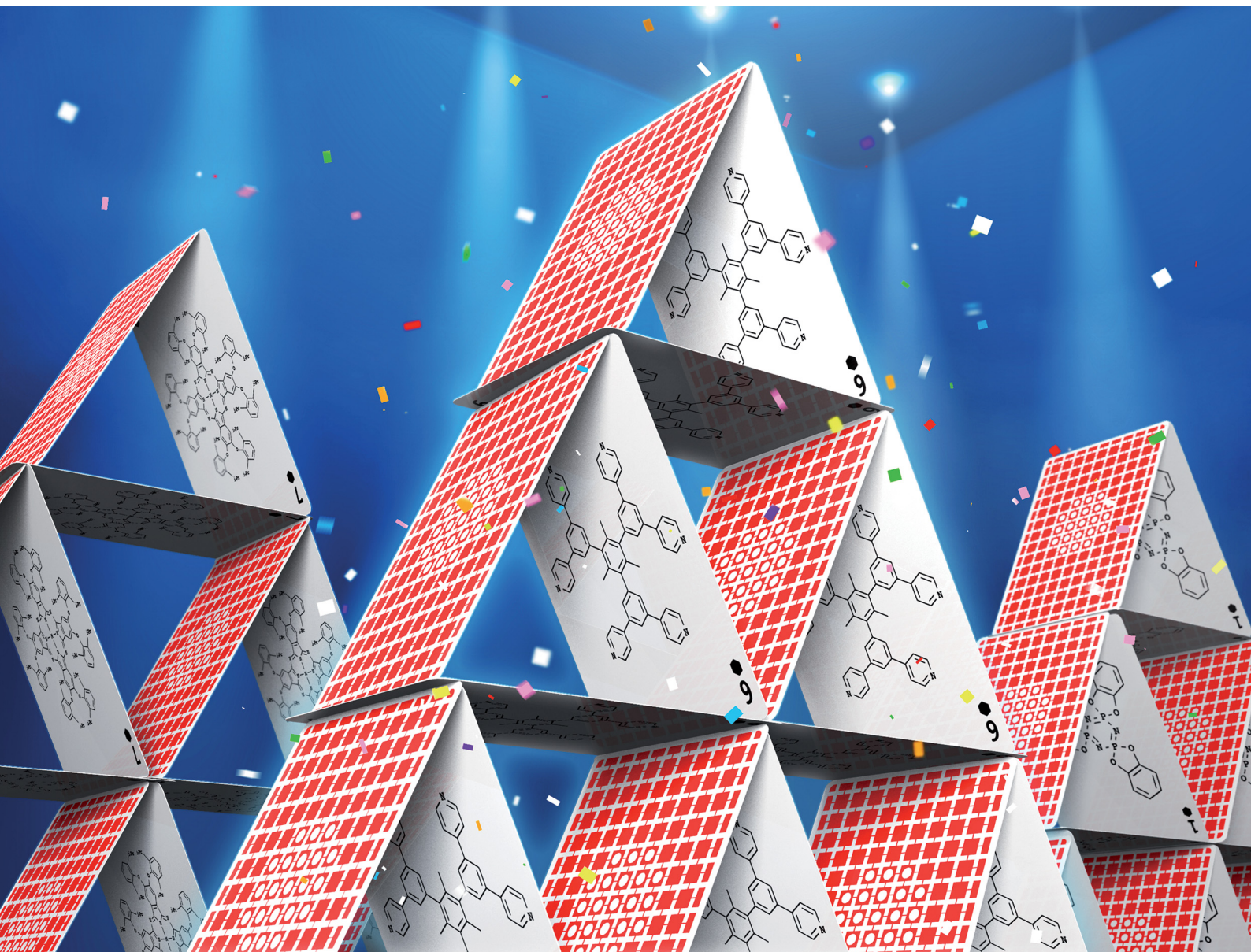


ChemComm

Chemical Communications

rsc.li/chemcomm



ISSN 1359-7345

FEATURE ARTICLE

Hiroshi Yamagishi
Functions and fundamentals of porous molecular crystals
sustained by labile bonds


 Cite this: *Chem. Commun.*, 2022, 58, 11887

Functions and fundamentals of porous molecular crystals sustained by labile bonds

 Hiroshi Yamagishi 

Organic molecules favour dense packing so that they can maximise the enthalpic gain upon solidification. Multidentate organic molecules that can form reticular bonding networks have been considered essential to overcome this tendency and assemble the molecules in a porous manner. Meanwhile, contrary to this understanding, a few organic molecules have been found to form porous molecular crystals by simply stacking with each other *via* van der Waals forces or analogous very weak noncovalent interactions. Although the porous molecular crystals were relatively rare in the 2000s due to the difficulty in the synthesis, their number has increased in the last decade, and their functional uniqueness has been unveiled eventually. This article reviews the recent advances in such functional porous molecular crystals. Particularly, thermal stability, processability, structural dynamicity, reactivity, and self-healing ability are highlighted. In addition, fundamental principles behind their functionalities, including the history, energetics, and the effect of crystallization solvent, are also reviewed.

 Received 26th August 2022,
Accepted 26th September 2022

DOI: 10.1039/d2cc04719e

rsc.li/chemcomm

1. Introduction

In the 1990s, a highly general methodology for making porous crystals from organic molecules was established.^{1–5} Researchers found that some rigid organic molecules, in conjunction with metal ions, assemble together *via* multiple coordination bonds and develop a porous crystalline framework that is

robust even after removal of the crystallisation solvent. The chemistry of porous organic crystals has been greatly expanded since then, and a variety of porous organic crystals have eventually been developed by using the reticular bonding strategy.

The most common classification of porous crystals is based on the type of chemical bonds utilised for connection of the constituent organic molecules. Porous crystals sustained completely by covalent bonds are the most classical, represented by zeolites.^{6,7} Covalently bonded porous crystals typically feature significant thermal and chemical stability and are utilised for many industrial applications. Metal–organic frameworks (MOFs) are hybrids of organic and inorganic metal compounds whose porous assembly is sustained by coordination bonds. MOFs feature relatively high thermal stability and wide compositional diversity. Dynamic covalent bonds, ionic bonds, and hydrogen bonds are likewise applicable for the synthesis of porous crystals.^{8–16}

The chemical bonds listed above are strong enough to prevent the collapse of the pores upon removal of the solvent molecules. Knowing this background, one may wonder whether porous crystals are available by using much weaker interactions such as van der Waals forces or weak hydrogen bonds (C–H···X bonds). These bonds are highly labile and less directional and have therefore been considered unsuitable for the synthesis of porous crystals. However, contrary to this understanding, in the long history of crystal engineering, some research groups occasionally found some organic molecules that spontaneously form a porous framework that is fully sustained by weak noncovalent interactions.^{17–34} Despite the lability of the intermolecular bonds, porous molecular crystals (PMCs)

Department of Materials Science, Faculty of Pure and Applied Sciences, and Tsukuba Research Center for Energy Materials Science (TREMS), University of Tsukuba 1-1-1 Tennodai, Tsukuba, Ibaraki, 305-8573, Japan.
E-mail: yamagishi.hiroshi.ff@u.tsukuba.ac.jp


Hiroshi Yamagishi

Hiroshi Yamagishi is an Assistant Professor at the Department of Materials Science, Faculty of Pure and Applied Sciences, University of Tsukuba. He has been a co-founder of MyQTech Inc. since 2022. He obtained his PhD degree in the Department of Chemistry and Biotechnology, School of Engineering, The University of Tokyo in 2018. After graduation, he joined the research group led by Prof. Yamamoto as an assistant professor. His research

focuses on supramolecular chemistry and crystal engineering in conjunction with the optical and laser properties.

can maintain their porous structure even after removal of the guest molecules.

PMCs are of fundamental interest because they are no different from classical molecular solids while they overcome the general tendency towards dense packing. Moreover, some of the recent PMCs feature unique chemical and physical functionalities that are completely distinct from those of the conventional porous crystals sustained by much stronger chemical bonds. Although the design and synthesis of PMCs are still difficult, an increasing number of functional PMCs have been recently reported. This article will review such unique functionalities realised with PMCs. In addition, the basic understanding of PMCs, including their history, molecular structures, and physical basis of their structural stability, will be reviewed before detailed explanations of functional PMCs are provided.

2. Basics of PMCs

2.1 General difficulty in making porous crystals

In general, organic molecules have a strong tendency towards dense packing. By maximising the packing efficiency, organic molecules can realise enhanced number of intermolecular contacts and more enthalpic gain. The tendency towards dense packing becomes even stronger when the solid is crystalline. Consequently, the synthesis of porous crystals has been difficult, and until the 1990s, available porous crystals were limited mostly to those made from inorganic compounds such as zeolites (aluminosilicate) and hexacyanoferrates.^{6,7,35}

Clathrate crystals represent how problematic the tendency towards dense packing is. Clathrates are crystalline solids consisting of host and guest molecules and ubiquitously appear in a variety of natural environments and synthetic processes. The host molecules pack in a porous arrangement and entrap the guest molecules in the pores, forming a dense crystal. Ideally, removing the entrapped guest molecules may provide a porous crystalline framework, but this vision has been barely successful. In the absence of the guest molecules, the host molecules cannot maintain their porous molecular arrangement and readily move towards the vacancies, yielding a densely packed nonporous crystal (Fig. 1).¹⁷

The discovery of MOFs by Prof. O. Yaghi and Prof. S. Kitagawa in the late 1990s provided a methodology to overcome this fundamental difficulty.^{1,2} The professors found that rigid

organic molecules with multiple metal-ligating groups, upon complexation with appropriate metal ions, provide coordination polymers with a reticular bonding network. The crystals initially contain solvent molecules inside the frameworks as guests. Notably, unlike traditional clathrate crystals, MOFs can maintain their structural integrity and vacant pores even after removal of the solvent molecules.

The superior structural stability of the framework is attributed to the rigidity of the constituent organic molecules and the tightness of the coordination bonds. The reticular bonding network freezes the thermal movement of the organic molecules at room temperature and prevents the organic molecules from moving to the voids. In later works, this reticular bonding strategy was successfully applied to a variety of multidentate organic molecules and metal ions, providing many MOFs featuring diverse structures and functions. Moreover, the material scope was further expanded by making the reticular bonding network from a series of reversible chemical bonds other than coordination bonds.¹⁴

2.2 Organic porous crystals sustained by noncovalent bonds

The development of zeolites, MOFs and more recent porous crystals represents a historic trend of porous crystals; the chemical bonds utilised for assembly of porous crystals become increasingly weaker.¹⁴ The strengths of chemical bonds commonly utilised in the field of porous crystals are shown in Fig. 2. The typical bond-dissociation energy of covalent bonds is greater than 150 kJ mol⁻¹.³⁶ The coordination bonds typically feature a bond energy greater than 100 kJ mol⁻¹.³⁷ The conventional hydrogen bonds are relatively strong, with strengths ranging from 17 to 170 kJ mol⁻¹.^{38,39}

The basic chemical and physical properties of porous crystals are largely underpinned by the bond strength.⁴⁰ Generally, strong bonds provide high thermal and chemical stability, while the processability, designability, and structural flexibility are attenuated. For instance, zeolites are traditional porous materials consisting of covalent bonds and exhibit excellent thermal stability. Conversely, the synthesis and processing of zeolites require harsh conditions due to the large formation and dissociation energies of the covalent bonds. They do not dissolve into a solvent and are therefore always treated as a powder. The structural and compositional variety of zeolites is limited because the porous framework is available only from aluminosilicate.

The compositional diversity and processability are improved when using coordination bonds. MOFs can be assembled from a large variety of organic ligands and metal ions, enabling virtually infinite types of structures and functionalities. This is one of the most significant advantages of MOFs and makes them industrially promising. A tailored MOF can differentiate a slight change in the chemical structure of the guest molecules, for instance, the difference between ethane and ethene, which is particularly beneficial in industry. The synthesis of MOFs is much easier than that of zeolites. MOFs can be assembled by simply mixing solutions containing organic linkers and metal ions at ambient temperature. The thermal stability of MOFs is

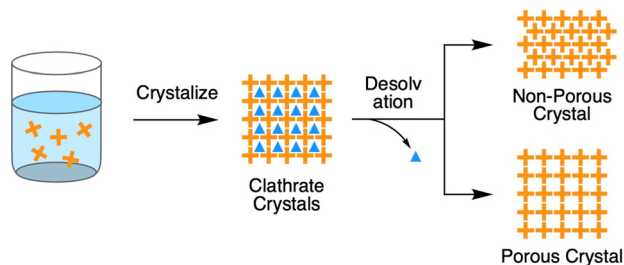


Fig. 1 Schematic illustrations of clathrate crystals and the conversion into porous/nonporous states via removal of guest molecules.

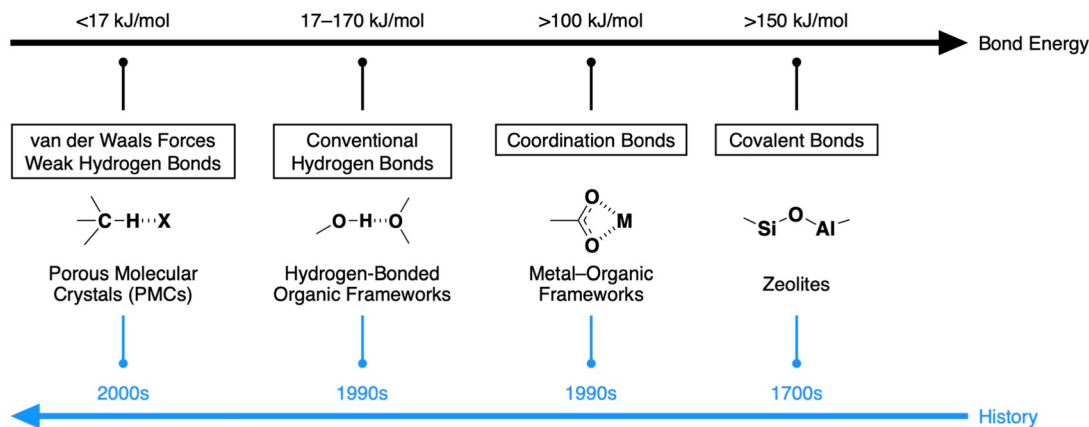


Fig. 2 Bond energy and history of porous crystals. Representative bond models are provided for each bond.

generally lower than that of zeolites but is still high among organic crystals.

Recently, porous crystals with further structural flexibility have been developed.^{41,42} Flexible MOFs are compositionally identical to typical MOFs, but flexible MOFs are unique in that they cannot maintain their porous framework in the absence of guest molecules because of the flexibility of the ligands and the metal coordination. The nonporous crystals are seemingly useless, but they can readily revert to the porous state when exposed to appropriate guest molecules. Since the gas-induced structural transition proceeds only with specific guest molecules, flexible MOFs are particularly beneficial for selective storage and separation from a mixture of organic compounds.

The chemical bonds utilised for assembly of porous organic crystals have been broadened to those with weaker strength than coordination bonds. Hydrogen-bonded organic frameworks (HOFs) have attracted attention along this line. The molecular strategy for assembling HOFs is basically analogous

to that for MOFs. The framework is assembled from discrete organic molecules that are bound to each other *via* multiple hydrogen bonds. The relatively weak bonding strength of the hydrogen bonds endows HOFs with good processability and solubility.⁴⁰ The crystallinity of HOFs is also high because error correction in the assembly process is highly facilitated by the reversible formation and cleavage of the hydrogen bonds. HOFs are available *via* simple procedures, such as evaporation of the solvent or cooling of supersaturated solutions, which are much milder than the procedures for MOFs.

2.3 Development of PMCs

Some researchers, including my group, found that noncovalent interactions weaker than conventional hydrogen bonds can sustain porous frameworks (Fig. 3). The applicable weak bonds include C-H...X bonds, π ... π interactions, halogen bonds, and van der Waals interactions. All these bonds are distinct from the other chemical bonds in several basic aspects.^{38,39,43–48} First, the

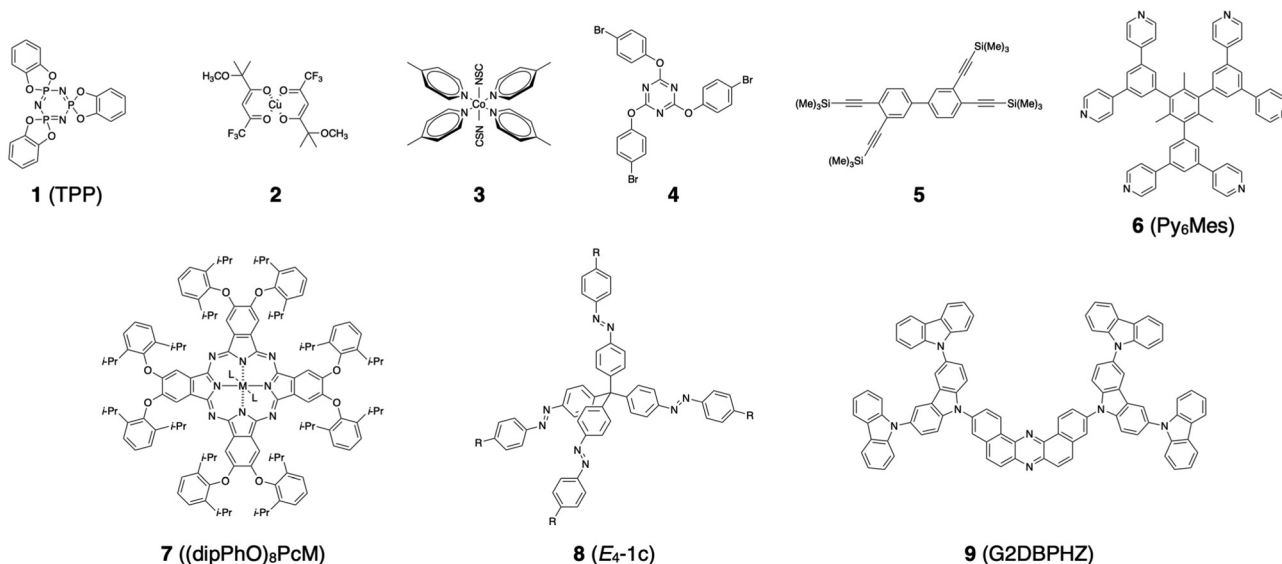


Fig. 3 Molecular structures of representative PMCs.

bonding strengths of these bonds are below 17 kJ mol^{-1} , which is much weaker than conventional hydrogen bonds such as $\text{O-H} \cdots \text{O}$ or $\text{N-H} \cdots \text{N}$. Second, the attractive force of these bonds originates mainly from the dispersion force rather than from dipole-dipole interactions. Therefore, these bonds are less directional than covalent, coordination, and conventional hydrogen bonds. Third, the response to the polarity of the surrounding medium is negligible in comparison to the other bonds. The nonpolar interactions are less affected by the surrounding polarity and therefore effective regardless of the polarity of the solvents. This property is well discussed in protein chemistry.⁴⁵

A molecular crystal of tris-*o*-phenylenedioxy-cyclotriphosphazene (TPP) is a historic PMC. Synthesis and crystallisation of TPP were originally conducted by Prof. H. R. Allcock, but the crystals reported by his group were mostly clathrates that could not be converted into a porous state.^{49–51} In 2005, Prof. P. Sozzani succeeded in obtaining a PMC from TPP by careful desolvation.¹⁸ The single-crystal structure features a highly symmetric hexagonal lattice, where TPP molecules interact with each other *via* weak $\text{C-H} \cdots \text{O}$ interactions. Prof. N. McKeown reported another PMC in 2009.²⁴ The group utilised a database provided by the Cambridge Crystallographic Data Centre and found an organic crystal that can maintain its framework without guest molecules. More detailed information about the early history of PMCs and representative molecules can be found in previous reviews.^{15,17,32}

The weakness of the intermolecular bonds endows PMCs with several potential benefits that are distinct from the other porous materials. For instance, PMCs feature significantly high processability. PMCs readily dissolve in organic solvents and can be retrieved through just simple drying of the solution, which is energy- and time-efficient in comparison with the

other crystallisation and recycling processes. Some molecules are sublimable and can be purified and deposited *via* gas phase. PMCs feature relatively high molecular dynamicity. The constituent molecules can move and oscillate with ease in the porous framework, enabling structural transitions triggered by mild external stimuli such as guest molecules, heat, and light. The weak bonds consist mainly of dispersion force that is robust regardless of the polarity of the surrounding media. This property endows PMCs with high chemical stability particularly in aqueous conditions, which is one of the major concerns with MOFs, covalent organic frameworks (COFs), and HOFs. The molecular design for PMCs is free from binding sites, such as imine bond and carboxylic acid. Therefore, the applicable molecular structures are diverse as found in the reported molecules thus far.

These unique features are of fundamental interest, but the thermal and chemical stability of PMCs is not high for many applications. Most PMCs are thermally less stable than MOFs and typically lose their porosity when heated at approximately 100°C . Moreover, modification of the molecular structure is virtually impossible. Even a slight change in substituents or the introduction of a functional group mostly results in the formation of densely packed crystals, which makes their further application difficult.

2.4 Energetics of porous crystals

A general understanding of the stability of porous frameworks and the energetic landscape of the structural transition was previously described by Y. Sakata *et al.* using a flexible MOF as a model (Fig. 4a).⁵² They considered three states. The initial state is the crystalline framework including guest molecules, the second state is the guest-free porous crystalline framework,

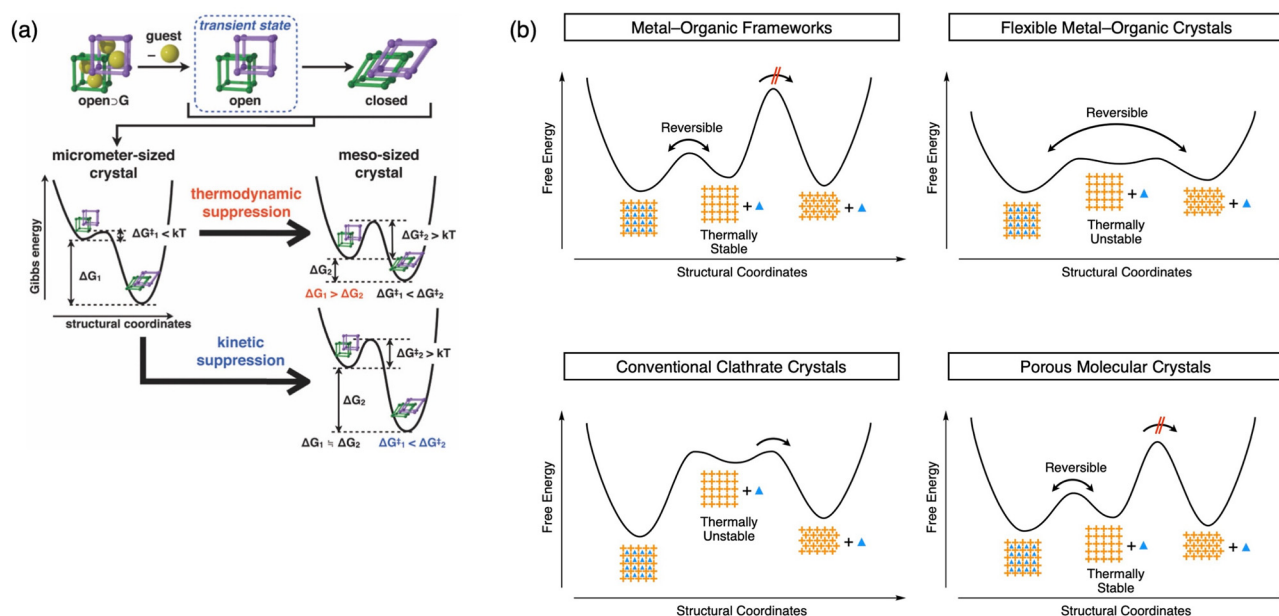


Fig. 4 Energy diagrams of the phase transitions of porous crystals. (a) Schematic representations of the energy landscape of a shape-memory MOF. The porous state becomes metastable by increasing the activation barrier or stabilising the porous state. Reproduced from ref. 52 with permission from AAAS, Copyright (2013). (b) Schematic representations of the energy landscape of porous crystals (MOFs, flexible MOFs, clathrate crystals, and PMCs).

and the final state is the dense form. Thermodynamically, the guest-free porous state is less stable than the dense state or the initial guest-filled state, and the crystals must overcome certain activation barriers during every structural transition. The thermal stability of each state is dominated by its thermodynamic stability and the activation barriers. The guest-free porous state is available at room temperature as a kinetically trapped state when the activation energy is sufficiently large relative to the thermal energy at room temperature. Otherwise, the crystal spontaneously transforms into the dense state. The activation barriers can be enhanced by using rigid organic molecules and strong bonding networks.

Fig. 4b shows schematic representations of the energetic landscapes of MOFs, flexible MOFs, conventional clathrate crystals, and PMCs. The free energies of the three states (porous state including guest molecules, porous state without guest molecules, and nonporous state) and the activation barriers between the three states determine the structural transition characteristics of the crystals. For instance, MOFs feature a very high activation barrier between the porous and nonporous states, which endows MOFs with high thermal stability. The activation barrier between the porous states with and without guests is low, enabling efficient gas sorption at ambient temperature. Flexible MOFs feature low activation barriers. Thus, flexible MOFs readily transform from the nonporous to guest-filled porous state *via* gas adsorption, and *vice versa*. The guest-free porous state is unavailable due to the very small activation barriers. Conventional clathrate crystals are highly stable when they incorporate guest molecules. The guest-free porous state is unavailable because the activation barrier towards the nonporous state is too small. Alternatively, a nonporous state is provided by the removal of the guest molecules. PMCs feature an energetic landscape similar to that of MOFs. The activation barrier towards the nonporous state is sufficiently high to make the guest-free porous form metastable at room temperature. This is noteworthy considering the weakness of the chemical bonds utilised in PMCs.

2.5 Solvophobicity as a driving force to assemble PMCs

In most cases, PMCs are found by chance. Researchers have yet to establish a reasonable theory regarding why these molecules

assemble in a porous manner rather than forming a dense nonporous polymorph. In 2021, we reported polymorphic behaviour of a porous crystal that may provide a clue to solve this fundamental question.³¹

The crystals were made from 1,3,5-trimethyl-2,4,6-tris(3,5-dipyrid-4-ylphenyl)benzene (**Py₆Mes**), which was previously reported to form a porous crystal **Py^{open}** ⊃ MeCN (the details of the molecule and the crystals are provided in Section 3.3). The polymorphs of **Py₆Mes** were synthesised by recrystallisation in a series of common organic solvents. The crystals formed in butyronitrile, EtOAc, and isopropanol are porous and isomorphous to **Py^{open}** ⊃ MeCN. In contrast, the crystals formed in acetone, 1-chloropropane, 1-butanol, tetrahydrofuran, CHCl₃, toluene, CH₂Cl₂, dimethylsulfoxide, and γ -butyrolactone are nonporous (Fig. 5a). The correlation of the polymorphic behaviour with several physical parameters was examined. Among them, Hansen solubility parameters explain the polymorphic behaviour well (Fig. 5b). The Hansen parameters consist of three indices representing the chemical affinity in terms of hydrogen bonds (δ_{H}), dipole interactions (δ_{P}), and dispersion force (δ_{D}). The polymorphs of **Py₆Mes** were plotted in the three-dimensional Hansen space based on the coordinates of the crystallisation solvents. In the three-dimensional space, we found two trends. The solvents close to **Py₆Mes** in the Hansen space provide nonporous polymorphs, and *vice versa*. In particular, δ_{D} shows the most straightforward correlation with the polymorphic behaviour. The solvents with small δ_{D} do not have affinity to **Py₆Mes** and form porous polymorphs, whereas the solvents with large δ_{D} have affinity to **Py₆Mes** and form nonporous crystals. The single-crystal structures of the polymorphs coincide with this tendency. Crystals formed in affinitive solvents (THF, CHCl₃, toluene, and CH₂Cl₂) include the crystallisation solvent molecules as guests. The guest molecules significantly interact with **Py₆Mes** by forming multiple atomic contacts, while the mutual contacts between **Py₆Mes** molecules are much less than those found in **Py^{open}**. In contrast, all the porous crystals formed in MeCN, iPA, and EtOAc show multiple mutual contacts between **Py₆Mes** molecules. In addition, blurred electron clouds that cannot be assigned to

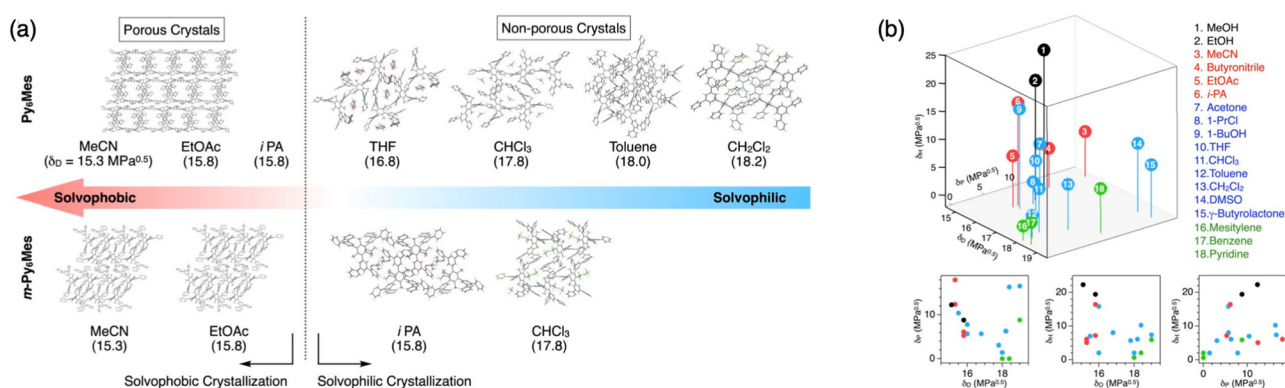


Fig. 5 Solvophobicity-directed polymorphism of PMCs. (a) Trend in the polymorphism of **Py₆Mes** and its derivative **m-Py₆Mes** as a function of δ_{D} (dispersion force component of the Hansen solubility parameters). (b) Three-dimensional plot of the crystallisation solvents in the Hansen space and its projections (bottom). Reproduced from ref. 31 with permission from Nature Portfolio, Copyright (2021).

atoms or molecules appear in the pores. The unassignable electron clouds indicate high mobility of the guest molecules in the pores and indicate lower interactions of the guest with the pore surface, which is consistent with the lower affinity of the guest molecules with **Py₆Mes**. This polymorphic tendency is further supported by *m*-**Py₆Mes**, which is an analogue of **Py₆Mes**.

These crystallographic studies provide a new solvophobicity-based theory about the polymorphism of PMCs. The solvents with large δ_D tend to interact with and intercalate between **Py₆Mes** molecules and form clathrate crystals, which are non-porous because the guest molecules fill the gap between **Py₆Mes** molecules. Removing the guest molecules from such clathrate crystals is thermally demanding, and the host framework is unstable when removing the guests because the crystal packing is stabilised largely by the interactions between the guest and host molecules rather than by the mutual interactions between the host molecules. In contrast, solvents with small δ_D cannot effectively interact with **Py₆Mes**. Therefore, **Py₆Mes** molecules assemble with one another so that the mutual interactions between **Py₆Mes** molecules are maximised. The resulting packing is not dense because **Py₆Mes** is a sterically bulky and spiky molecule, but such inefficient packing is favourable for maximising the mutual contact of **Py₆Mes** molecules. Namely, the porous framework is provided by the solvophobic effect. The pores are initially filled with the guest solvent, but the guest molecules barely interact with the pore surface and readily escape from the pores when dried. Since the porous framework is stabilised not by the host-guest interactions but by the host-host interactions, the porous assembly remains intact even after removal of the guest molecules.

2.6 Molecular crystals with intrinsic microporosity

Porous crystals made from cyclic molecules are another promising candidate to expand this field. These crystals are typically termed crystals of “intrinsic porosity”, while the aforementioned crystals are termed crystals of “extrinsic porosity”. The intrinsic porosity is realised by interconnection of the cavities of the constituent cyclic molecules. The molecular strategy of intrinsic porosity seems much simpler than that of extrinsic porosity, but the synthesis of crystals with intrinsic pores has been difficult. Almost all the molecular crystals of cyclic molecules are nonporous due to the inappropriate packing or the contraction of the macrocycles upon removal of the crystallisation solvents.

The discovery of cage molecules by Prof. A. I. Cooper changed this situation.^{53–56} The cages assemble into molecular crystals such that the open windows of the cages engage with each other to form continuous pores. The cages are rigid and maintain the porous assembly even after removal of the solvents. Unlike PMCs with extrinsic porosity, many derivatives of the cages form porous crystals and enable on-demand functionalisation of the pores. By taking this advantage, the group successfully reported, for instance, asymmetric porous crystals, predictable porous crystals, porous liquid, and porous membrane for isotope separation.^{54,56–58} The details of the cage

molecules and their crystals will not be reviewed in this article because the basic principles for designing and making these crystals are different from those of intrinsic micropores.

3. Functional PMCs

Since the first PMCs were developed, the gas storage and separation properties have been the primary research targets.¹⁸ Some PMCs can adsorb N₂ and CO₂, but improvement of the gas adsorption properties has been difficult. This is because PMCs are extremely sensitive to modification of the molecular structure. Even a slight change in the molecular structure results in the formation of nonporous crystals. For instance, Allcock *et al.* synthesised analogues of TPP, but none of them formed PMCs.⁵¹ Designing PMCs with unique functions other than gas sorption is an even more difficult task. Nonetheless, several functional PMCs have recently been discovered, which will be introduced in the following sections.

3.1 Thermally stable PMCs

In 2019, Prof. N. McKeown *et al.* reported a PMC with exceptionally high thermal stability.²⁶ This is an extension of their previous report on a molecular crystal made from a phthalocyanine derivative ((dipPhO)₈PcM, Fig. 6a).²⁵ In the previous report, the authors reported that the PMC belongs to the space group *Pr $\bar{3}$ n* and features a large cavity. The cavities of the as-synthesised crystal are filled with the crystallisation solvents and readily collapse after removal of the crystallisation solvents unless (dipPhO)₈PcM molecules are connected to each other *via* metal-ligating organic linkers.

In the recent work, the authors revealed that the pores of the (dipPhO)₈PcM crystal are perfect in size and shape for the inclusion of a fullerene molecule and found that (dipPhO)₈PcM

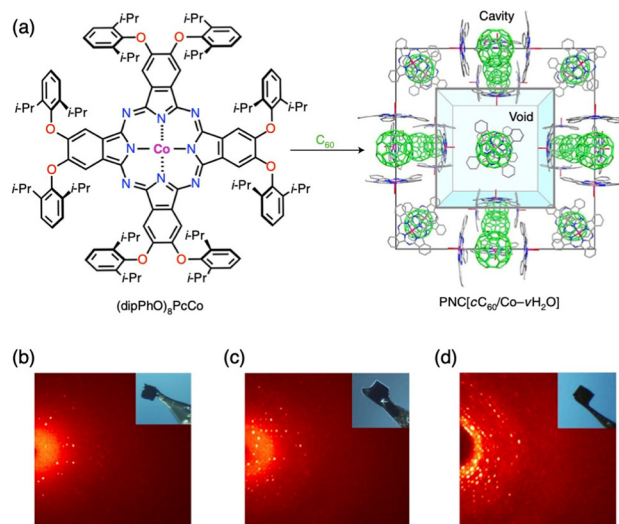


Fig. 6 Thermally stable PMC. (a) Molecular structure and crystal packing diagram. (b–d) Diffraction spots obtained from single crystals after soaking in boiling water (b), boiling aqueous NaOH solution (c), and boiling aqueous HCl solution (d). Reproduced from ref. 26 with permission from Nature Portfolio, Copyright (2019).

and the fullerene C₆₀ or C₇₀ cocrystallise to form PMCs (Fig. 6a). The guest fullerene molecules occupy some of the cavity and leave some continuous pores. The crystallisation solvent included in the cocrystals was removed by exposing the crystals to a stream of N₂ gas at room temperature. The evacuated cocrystals are porous, as proven by the N₂ adsorption isotherms at 77 K. The Brunauer–Emmett–Teller (BET) surface area is 970 m² g⁻¹, and the pore volume is 0.46 mL g⁻¹.

The cocrystals are stable even under a high hydrostatic pressure. The cocrystal with C₆₀ maintains good crystallinity under pressures up to 3.9 GPa and transforms into an amorphous state under pressures above 4.5 GPa. The mechanical stability of the cocrystal is higher than that of conventional rigid MOFs and is comparable to that of the most stable MOFs. The thermal stability of the cocrystal measured by variable-temperature powder X-ray diffractometry (PXRD) is above 500 K, which is exceedingly high as a PMC. The cocrystals are stable even to hydrolytic treatments (Fig. 6b–d). The crystals were immersed in water, aqueous 2 M NaOH and aqueous 2 M HCl solutions at 100 °C for 24 h. The cocrystals survived all the harsh conditions and maintained their single crystallinity. The robustness against hydrolytic conditions is attributed to the nonpolar nature of the van der Waals interactions.

3.2 Nonporous-to-porous structural transition of PMCs

Prof. J. L. Atwood *et al.* reported in 2010 the regeneration of a porous framework from a nonporous polymorph by gas adsorption (Fig. 7a).⁵⁹ The group had long been interested in the structural transformations of molecular crystals triggered by ambient stimuli and previously found a molecular crystal that can adsorb guest gaseous molecules deep inside the solid even though the crystal features no continuous pores.^{60–62} They conjectured that the thermal vibration of the constituent molecules in the crystal allows the small guest molecules to permeate into the crystal.

In a paper published in 2010, they reported an analogous but very intriguing structural transition of TPP. TPP exists in two polymorphic forms (guest-free porous state and nonporous state). The porous polymorph is a kinetically formed metastable state, and the nonporous polymorph is a thermodynamically favoured stable state, which is obtained by thermal annealing of the porous polymorph or sublimation of TPP. They found that the nonporous crystal spontaneously transforms into a porous state with the adsorption of CO₂. The PXRD profile of the crystal obtained under a pressurised CO₂ atmosphere proved the transition into the porous phase. The reaction time to complete the transition depends on the CO₂ pressure. For instance, the transition under a pressure of 350 psi was completed in 3 hours, while that under a pressure of 150 psi was completed in 2 days. During the structural transition, the crystals uptake 12 wt% CO₂, which coincides with the pore volume of the porous polymorph (Fig. 7b). The guest CO₂ molecules adsorbed in the pores autonomously escape from the pores upon release of the gas pressure, leaving a metastable guest-free porous polymorph.

The same phase transition can be achieved with N₂O but not with H₂ or helium. This implies that the chemical affinity of the

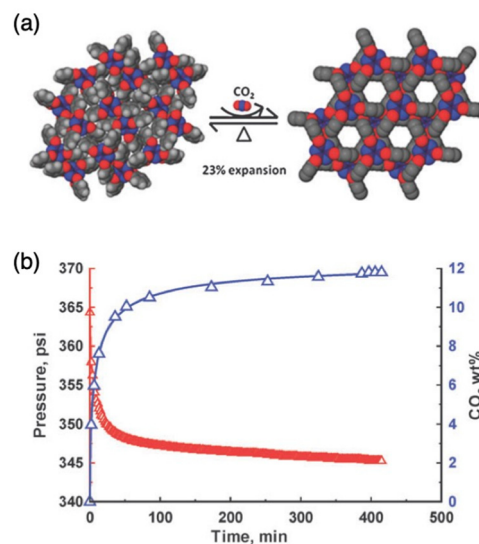


Fig. 7 Nonporous-to-porous structural transition of a PMC. (a) Schematic representation of the reversible structural transition of TPP between the porous and nonporous states. (b) Conversion of the crystal from nonporous to porous at 298 K as a function of gas loading and time. Reproduced from ref. 59 with permission from RSC, Copyright (2011).

guest molecules and the pore surface is the driving force of the phase transition from the thermally stable nonporous to metastable porous forms. This is the first finding of regeneration of the porous form of PMCs without dissolving the crystals.

3.3 Thermally stable and self-healable PMCs

In 2018, our group reported a PMC featuring both high thermal stability and self-healing ability.²⁸ We designed and synthesised a novel mesitylene derivative **Py₆Mes** without any intention to make a PMC. **Py₆Mes** is a D_{3h}-symmetric sterically bulky molecule (Fig. 8b). The peripheral 3,5-dipyrid-4-ylphenyl blades tilt almost perpendicular to the central mesitylene due to the steric repulsion with the methyl groups at the mesitylene. During the synthesis, we purified **Py₆Mes** by recrystallisation in MeCN and occasionally found a PMC made from **Py₆Mes**. The porous crystal (**Py^{open}**) belongs to the space group *P2₁/c*, and **Py₆Mes** molecules assemble *via* C–H···N and C–H···π interactions to form columnar stacking along the crystallographic 2-fold screw axis. The columns form two-dimensional sheets on the crystallographic *bc* plane, in which one-dimensional pores with an average pore diameter of 6 Å form. The porous sheets stack on top of one another along the crystallographic *a* axis. The pores of the as-synthesised crystal (**Py^{open} ⊃ MeCN**) are filled with the MeCN solvent molecules, but the MeCN molecules do not strongly adhere to the pore surface and are gradually and autonomously released into the surrounding atmosphere at room temperature. **Py^{open}** after removal of the solvent molecules is thermally stable and maintains the porous structure up to 202 °C.

Heating at a temperature higher than 202 °C induces the structural phase transition of **Py^{open}** to the nonporous polymorph **Py^{close}**. **Py^{close}** is thermodynamically more stable than

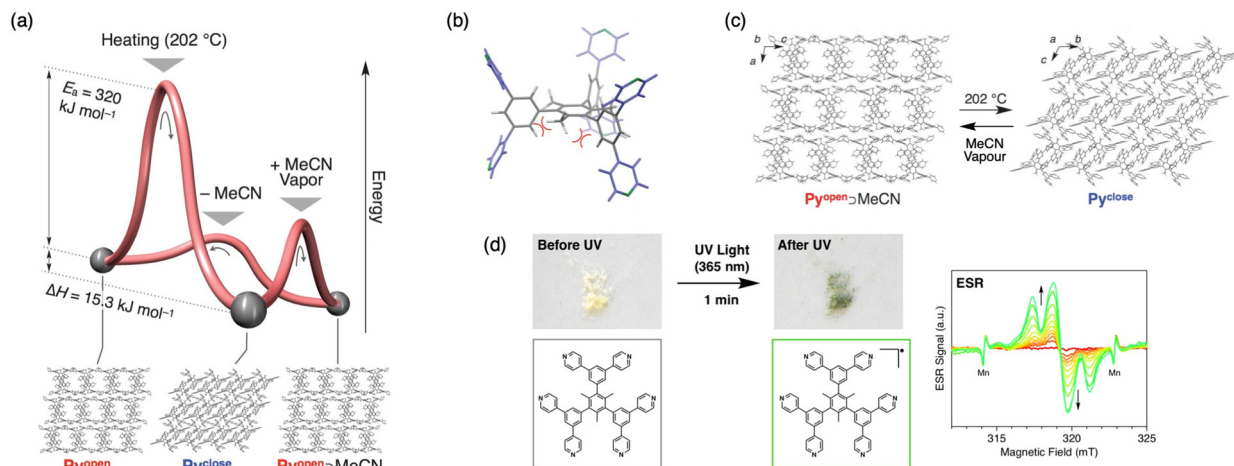


Fig. 8 Thermally stable and self-healable PMC. (a) Schematic illustration of the phase transitions between $\text{Py}^{\text{open}} \supset \text{MeCN}$, Py^{open} , and Py^{close} . (b) Molecular structure of Py_6Mes . (c) Crystal packing diagrams of $\text{Py}^{\text{open}} \supset \text{MeCN}$ and Py^{close} , and external stimuli for inducing the structural transition. (d) Photographs of powder specimens of Py^{open} soaked in an aqueous solution of TEABF_4 before and after UV light irradiation together with the corresponding ESR spectra. Reproduced from ref. 28 and 29 with permission from AAAS and RSC, Copyright (2018 and 2020).

Py^{open} and does not revert to Py^{open} after cooling to room temperature. Intriguingly, Py^{close} autonomously transforms to $\text{Py}^{\text{open}} \supset \text{MeCN}$ when exposed to MeCN vapour at room temperature for 7 hours (Fig. 8c). This healing process does not proceed when using an amorphous solid of Py_6Mes as a starting material, indicating that the arrangement of Py_6Mes in the initial state is important to achieve the backward structural transition.

The high thermal stability and healing ability of Py^{open} are of fundamental interest because structural stability and healing ability are typically incompatible, which is evident from the structural transition of flexible MOFs described above. To elucidate the mechanism, we quantitatively measured the energetic barriers of the structural transitions (Fig. 8a). The barrier from Py^{open} to Py^{close} is 320 kJ mol^{-1} , which is much larger than the thermal energy at room temperature and is consistent with its thermal robustness. In clear contrast, the healing process from Py^{close} to $\text{Py}^{\text{open}} \supset \text{MeCN}$ proceeds at ambient temperature, whose thermal energy is typically considered to be approximately 100 kJ mol^{-1} . Namely, Py^{open} features a high activation barrier in the pore closing process, while the barrier in the pore recovery process is largely reduced. The underlying molecular mechanism for the high thermal robustness and self-healing ability is still under investigation.

3.4 Photochemical radical generation in PMCs

Organic compounds that can generate radical species in response to light irradiation find unique applications in materials science. They are distinct from permanent organic radicals in that their radical nature can be spatiotemporally switched on and off. Generation of radicals in porous crystals is further attractive in view of electronics because porous frameworks can act as conductive electrodes with a large specific surface area. However, the current molecular design scope towards this end is limited because of the difficulty in developing novel organic precursors that are stable even after *in situ* one-electron reduction/oxidation

induced by photoirradiation and that are applicable for construction of porous crystals.

In 2020, our group reported that Py^{open} can generate stable radicals upon light irradiation (Fig. 8d).²⁹ Prior to irradiation with light, Py^{open} is immersed in an aqueous solution of tetraethylammonium tetrafluoroborate (TEABF_4). After 20 hours, the crystalline powder is collected and dried under reduced pressure for 2 hours. The amount of TEABF_4 incorporated in Py^{open} is 91 mol% relative to Py_6Mes . The water content in Py^{open} is 2.2 wt%, which is more than double the water uptake of pristine Py^{open} . Upon irradiation with UV light (365 nm) for 1 min, the colour of Py^{open} changes from pale yellow to green, which is due to the emergence of a new absorption peak at 710 nm in the diffuse reflectance spectra. In the electron spin resonance (ESR) spectra, the green powder shows a broadened triplet signal with a g value of 2.00281, which is assignable to the pyridinyl radical according to a previous report.⁶³ The hyperfine structure indicates the interaction of the unpaired electron with the nitrogen atom in the pyridine ring, and the broadening of the signal indicates delocalisation of the electron around the pyridine and proximal phenyl rings. The photo-generated radical species survive for a long time (half-life of 3.5 min) even in the presence of water and oxygen at room temperature, which is exceedingly high among reported pyridyl radicals. The radical contents gradually decrease in several minutes but can be re-enriched by irradiation with UV light. The developed methodology is facile and will contribute to further electric functionalisation of PMCs in the future.

3.5 Photochemical phase transition of PMCs

In 2015, Prof. A. Credi *et al.* reported a PMC with porosity that can be switched *via* photoisomerisation reactions.²⁷ The newly designed and synthesised tetraphenylmethane derivative bearing an azobenzene unit at each phenyl arm ($E_4\text{-1c}$) crystallises in the tetragonal system. The central tetrahedral node of $E_4\text{-1c}$ lies on a crystallographic 4-fold rotoinversion axis, and the

rotoinversion operations along the axis generate the four phenyl arms. The E_4-1c molecules stack on top of one another along the crystallographic c -axis, and the columns pack in an antiparallel manner, leaving a continuous 1-dimensional pore between the adjacent four columns (Fig. 9a). Isostructural tetragonal crystals are obtained when analogues of tetraphenylmethane featuring sterically less bulky terminal groups are applied, which is a rare case among PMCs, although the porosity mostly diminishes when using smaller termini. Detailed molecular interactions or contacts in the crystals are unavailable plausibly because of the low quality of the diffraction data and the associated large uncertainty in the crystal structure.

The azobenzene moieties of E_4-1c photoisomerise when subjected to 365 nm irradiation both in the solution and solid states. UV light induces E -to- Z isomerisation with an initial quantum yield of 0.18 and a conversion of >95% in the solution state. In the solid film state, the same photoisomerisation reaction proceeds with a yield of 32%. The backward isomerisation analogously proceeds under irradiation with 436 nm light or heating at 130 °C for 10 min. PXRD profiles and polarised optical microscopy (POM) images of film specimens of E_4-1c revealed the spatiotemporal phase transition of E_4-1c from crystalline to amorphous associated with the photoisomerisation reactions (Fig. 9c). Upon UV irradiation, both the birefringence in POM images and the diffraction peaks in PXRD profiles

disappear. The transition proceeds only in areas irradiated by the light. Heating the sample at 160 °C for 20 min induces the amorphous-to-crystal backward phase transition and regenerates the birefringence and the diffraction peaks of the specimens. This phase transition can be repeated in the same sample without degradation of the material.

The PMC consisting of the all- E isomer of E_4-1c shows a type-I sorption profile in the CO_2 adsorption isotherm measured at 195 K. In contrast, the crystal consisting of the all- Z isomer is not porous and shows negligible CO_2 uptake (Fig. 9b), demonstrating successful reversible switching between the porous and nonporous states induced by photoirradiation and heating.

3.6 Hydrochromic PMCs

In 2021, our group reported a PMC that exhibits a chromic behaviour associated with the uptake and release of H_2O molecules (Fig. 10b).³⁰ In the course of research on electrically functional dendrimers, we designed and synthesised a novel aromatic molecule consisting of a dibenzophenazine core and two second-generation carbazole dendrons (3,11-bis(9'- H -[9,3':6',9''-tercarbazol]-9'-yl)dibenzo[a_j]phenazine, **G2DBPHZ**, Fig. 10a). Mixing a $CHCl_3$ solution of **G2DBPHZ** with MeOH initially gave yellow amorphous precipitates of **G2DBPHZ**, which eventually turned red when standing at room temperature for several weeks. The red precipitate (**VPC-1^{red}**) is a crystalline powder featuring micropores with an average pore diameter of 5.6 Å; however, X-ray single-crystal structure analysis was unsuccessful, and the crystal structure is unknown.

VPC-1^{red} is a solvatochromic porous crystal. The colour of **VPC-1^{red}** changes when immersed in poor solvents, depending on the polarity of the solvent. The colour of **VPC-1** in H_2O is red, while it becomes yellow in hexane. The change in colour shows

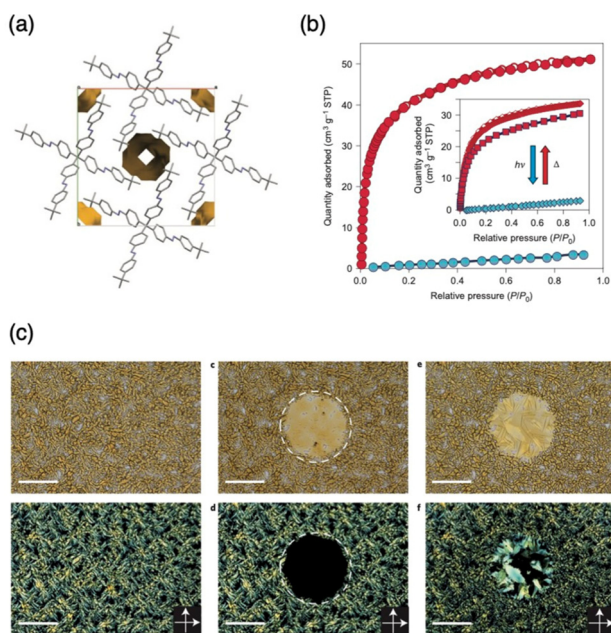


Fig. 9 Photoswitchable PMC. (a) Crystal packing diagram of E_4-1c . The pore geometry is visualised as yellow surfaces. (b) CO_2 adsorption isotherm of E_4-1c at 195 K before and after the isomerisation reactions. Nonporous-to-porous structural transition of the PMC. (c) POM images of E_4-1c under bright field (top) and cross-polarised (bottom) light illumination before (left) and after (middle) near-UV irradiation in the central spot, and photographs of the same area upon thermal annealing (right). Reproduced from ref. 27 with permission from Nature Portfolio, Copyright (2015).

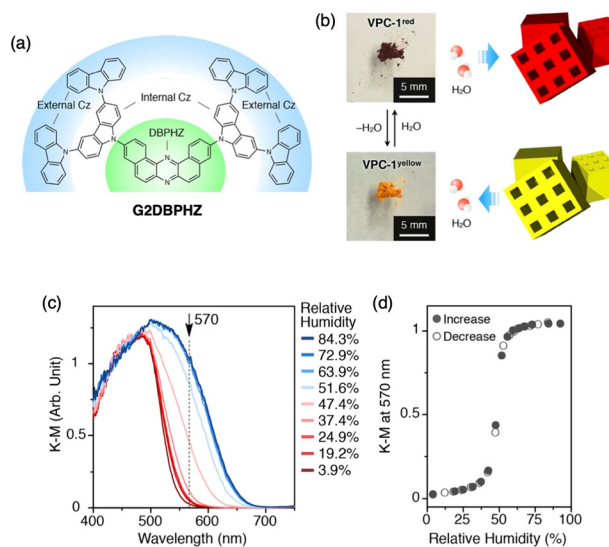


Fig. 10 Hydrochromic PMC. (a) Molecular structure of **G2DBPHZ**. (b) Photographs of **VPC-1^{red}** and **VPC-1^{yellow}**. (c) and (d) Diffuse reflectance spectra of **VPC-1** measured with variable RH (c), and corresponding plot of the $K-M$ values at 570 nm as a function of RH (d). Reproduced from ref. 30 with permission from Nature Portfolio, Copyright (2020).

a linear slope in the E_T30 plot, proving that the bandgap of **VPC-1^{red}** is largely affected by the polarity of the guest solvent.⁶⁴ H_2O is a suitable solvent for maximising the energetic stabilisation and induces the most significant redshift of the absorption band of **VPC-1**. This chromic behaviour is also visible even when the guest H_2O is provided as a vapour. The guest-free crystal (**VPC-1^{yellow}**) obtained by drying **VPC-1^{red}** under a reduced pressure appears yellow at a relative humidity (RH) of 0%. The colour of **VPC-1^{yellow}** suddenly turns red when the RH surpasses 50% at 25 °C. The vapochromism is consistently supported by diffusion reflectance spectroscopy, infrared (IR) absorption spectroscopy, and H_2O absorption isotherms, all of which show sigmoidal curves with a threshold of 50% RH (Fig. 10c and d).

PXRD and IR spectroscopy indicate molecular conformational transitions during H_2O sorption, particularly at the threshold RH. The 2θ values of all distinguishable peaks in the PXRD profiles of **VPC-1^{red}** and **VPC-1^{yellow}** are identical, while the intensities of some peaks are attenuated upon H_2O adsorption. These changes indicate that the crystal lattice of **VPC-1^{red}** remains intact throughout H_2O sorption, while certain conformational motions of **G2DBPHZ** are activated. The IR spectra of **VPC-1^{red}** and **VPC-1^{yellow}** show consistent humidity-dependent changes. A computational study revealed that the change in IR spectra is attributed to the rotational motion of the outermost carbazole units of **G2DBPHZ**, meaning that **VPC-1^{red}** is a partially flexible porous crystal featuring a stable porous framework and mobile peripheral units.

4. Perspective

To summarise, PMCs are distinct from the other conventional porous crystals in that the crystalline frameworks are sustained by labile noncovalent interactions. The lability of the intermolecular bonds largely affects the fundamental physical and chemical properties of the crystal. The major differences include the available molecular structures, polarity of the constituent molecules, and assembly pathway for constructing porous frameworks. In addition, PMCs feature unique functions, such as structural flexibility, stimuli responsiveness, processability, and robustness against aqueous conditions.

The chemistry of PMCs is still immature. The number of PMCs is still limited, and the available functionalities are not highly sophisticated. The essential difficulty in developing functional PMCs is the lack of a molecular strategy to assemble PMCs from discrete molecules. The reported PMCs were in most cases found by chance, and their molecular structures are completely different from each other. Moreover, even a slight change in the molecular structure drastically alters the packing regime of the crystals and provides nonporous polymorphs. A clearer molecular design strategy will change this situation and rapidly expand the field. Complex functionalisation of the crystals will follow once the strategy is established. Several groups, including us, are tackling this topic.

In conclusion, the field of PMCs has been ascending in the last two decades. The available compounds are still limited due

to the lack of a molecular strategy, but some PMCs with unique properties have been recently reported, promising a fruitful future of this field. Research on PMCs will surely expand the field of materials chemistry and contribute to deepening the fundamental understanding of molecular assembly.

Conflicts of interest

There are no conflicts to declare.

Acknowledgements

This work was supported by Grants-in-Aid for Scientific Research on Young Scientists (JP19K15334, JP22K14656) from the Japan Society for the Promotion of Science (JSPS) and New Energy and Industrial Technology Development Organization (NEDO).

Notes and references

- S. Kitagawa, R. Kitaura and S. Noro, *Angew. Chem., Int. Ed.*, 2004, **43**, 2334–2375.
- O. M. Yaghi, M. O'Keeffe, N. W. Ockwig, H. K. Chae, M. Eddaoudi and J. Kim, *Nature*, 2003, **423**, 705–714.
- J. L. C. Rowsell and O. M. Yaghi, *Microporous Mesoporous Mater.*, 2004, **73**, 3–14.
- H. Furukawa, K. E. Cordova, M. O'Keeffe and O. M. Yaghi, *Science*, 2013, **341**, 1230444.
- M. Kondo, T. Yoshitomi, K. Seki, H. Matsuzaka and S. Kitagawa, *Angew. Chem., Int. Ed. Engl.*, 1997, **36**, 1725–1727.
- C. S. Cundy and P. A. Cox, *Chem. Rev.*, 2003, **103**, 663–702.
- R. Millini and G. Bellussi, in *Zeolites in Catalysis*, The Royal Society of Chemistry, 2017, ch. 1, pp. 1–36.
- A. P. Cote, A. I. Benin, N. W. Ockwig, M. O'Keeffe, A. J. Matzger and O. M. Yaghi, *Science*, 2005, **310**, 1166–1170.
- S. Y. Ding and W. Wang, *Chem. Soc. Rev.*, 2013, **42**, 548–568.
- C. S. Diercks and O. M. Yaghi, *Science*, 2017, **355**, eaal1585.
- T. Miyano, N. Okada, R. Nishida, A. Yamamoto, I. Hisaki and N. Tohnai, *Chem. – Eur. J.*, 2016, **22**, 15430–15436.
- A. Yamamoto, T. Hasegawa, T. Hamada, T. Hirukawa, I. Hisaki, M. Miyata and N. Tohnai, *Chem. – Eur. J.*, 2013, **19**, 3006–3016.
- R. B. Lin, Y. He, P. Li, H. Wang, W. Zhou and B. Chen, *Chem. Soc. Rev.*, 2019, **48**, 1362–1389.
- I. Hisaki, C. Xin, K. Takahashi and T. Nakamura, *Angew. Chem., Int. Ed.*, 2019, **58**, 11160–11170.
- M. Mastalerz, *Chem. – Eur. J.*, 2012, **18**, 10082–10091.
- X. Song, Y. Wang, C. Wang, D. Wang, G. Zhuang, K. O. Kirlikovali, P. Li and O. K. Farha, *J. Am. Chem. Soc.*, 2022, **144**, 10663–10687.
- N. B. McKeown, *J. Mater. Chem.*, 2010, **20**, 10588–10597.
- P. Sozzani, S. Bracco, A. Comotti, L. Ferretti and R. Simonutti, *Angew. Chem., Int. Ed.*, 2005, **44**, 1816–1820.
- A. Y. Manakov, D. V. Soldatov, J. A. Ripmeester and J. Lipkowski, *J. Phys. Chem. B*, 2000, **104**, 12111–12118.
- D. V. Soldatov, J. A. Ripmeester, S. I. Shergina, I. E. Sokolov, A. S. Zanina, S. A. Gromilov and Y. A. Dyadin, *J. Am. Chem. Soc.*, 1999, **121**, 4179–4188.
- D. V. Soldatov, G. D. Enright and J. A. Ripmeester, *Cryst. Growth Des.*, 2004, **4**, 1185–1194.
- K. Reichenbacher, H. I. Süß, H. Stoeckli-Evans, S. Bracco, P. Sozzani, E. Weber and J. Hulliger, *New J. Chem.*, 2004, **28**, 393–397.
- K. Reichenbacher, G. Couderc, A. Neels, K. Krämer, E. Weber and J. Hulliger, *J. Inclusion Phenom. Macrocyclic Chem.*, 2008, **61**, 127–130.
- K. J. Msayib, D. Book, P. M. Budd, N. Chaukura, K. D. Harris, M. Helliwell, S. Tedds, A. Walton, J. E. Warren, M. Xu and N. B. McKeown, *Angew. Chem., Int. Ed.*, 2009, **48**, 3273–3277.

- 25 C. G. Bezzu, M. Helliwell, J. E. Warren, D. R. Allan and N. B. McKeown, *Science*, 2010, **327**, 1627–1630.
- 26 C. G. Bezzu, L. A. Burt, C. J. McMonagle, S. A. Moggach, B. M. Kariuki, D. R. Allan, M. Warren and N. B. McKeown, *Nat. Mater.*, 2019, **18**, 740–745.
- 27 M. Baroncini, S. d'Agostino, G. Bergamini, P. Ceroni, A. Comotti, P. Sozzani, I. Bassanetti, F. Grepioni, T. M. Hernandez, S. Silvi, M. Venturi and A. Credi, *Nat. Chem.*, 2015, **7**, 634–640.
- 28 H. Yamagishi, H. Sato, A. Hori, Y. Sato, R. Matsuda, K. Kato and T. Aida, *Science*, 2018, **361**, 1242–1246.
- 29 A. Nakayama, H. Kimata, K. Marumoto, Y. Yamamoto and H. Yamagishi, *Chem. Commun.*, 2020, **56**, 6937–6940.
- 30 H. Yamagishi, S. Nakajima, J. Yoo, M. Okazaki, Y. Takeda, S. Minakata, K. Albrecht, K. Yamamoto, I. Badia-Dominguez, M. M. Oliva, M. C. R. Delgado, Y. Ikemoto, H. Sato, K. Imoto, K. Nakagawa, H. Tokoro, S. Ohkoshi and Y. Yamamoto, *Commun. Chem.*, 2020, **3**, 118.
- 31 H. Yamagishi, M. Tsunoda, K. Iwai, K. Hengphasatporn, Y. Shigeta, H. Sato and Y. Yamamoto, *Commun. Chem.*, 2021, **4**, 122.
- 32 J. Tian, P. K. Thallapally and B. P. McGrail, *CrystEngComm*, 2012, **14**, 1909–1919.
- 33 J. R. Holst, A. Trewin and A. I. Cooper, *Nat. Chem.*, 2010, **2**, 915–920.
- 34 M. A. Little and A. I. Cooper, *Adv. Funct. Mater.*, 2020, **30**, 1909842.
- 35 L. J. M. Coleby, *Ann. Sci.*, 1939, **4**, 206–211.
- 36 S. J. Blanksby and G. B. Ellison, *Acc. Chem. Res.*, 2003, **36**, 255–263.
- 37 M. M. Raikhshtat and V. V. Zhogina, *J. Struct. Chem.*, 1995, **36**, 333–337.
- 38 T. Steiner, *Angew. Chem., Int. Ed.*, 2002, **41**, 49–76.
- 39 G. R. Desiraju, *Acc. Chem. Res.*, 2002, **35**, 565–573.
- 40 J. Yang, J. Wang, B. Hou, X. Huang, T. Wang, Y. Bao and H. Hao, *Chem. Eng. J.*, 2020, **399**, 125873.
- 41 Y. Wan and D. Zhao, *Chem. Rev.*, 2007, **107**, 2821–2860.
- 42 A. Schneemann, V. Bon, I. Schwedler, I. Senkovska, S. Kaskel and R. A. Fischer, *Chem. Soc. Rev.*, 2014, **43**, 6062–6096.
- 43 T. Steiner and G. R. Desiraju, *Chem. Commun.*, 1998, 891–892, DOI: [10.1039/a708099i](https://doi.org/10.1039/a708099i).
- 44 G. R. Desiraju, *Angew. Chem., Int. Ed.*, 2007, **46**, 8342–8356.
- 45 M. Nishio, *CrystEngComm*, 2004, **6**, 130–158.
- 46 M. Nishio, Y. Umezawa, K. Honda, S. Tsuboyama and H. Suezawa, *CrystEngComm*, 2009, **11**, 1757–1788.
- 47 M. Mascal, *Chem. Commun.*, 1998, 303–304, DOI: [10.1039/a707702e](https://doi.org/10.1039/a707702e).
- 48 L. C. Gilday, S. W. Robinson, T. A. Barendt, M. J. Langton, B. R. Mullaney and P. D. Beer, *Chem. Rev.*, 2015, **115**, 7118–7195.
- 49 H. R. Allcock, *J. Am. Chem. Soc.*, 1963, **85**, 4050–4051.
- 50 H. R. Allcock and L. A. Siegel, *J. Am. Chem. Soc.*, 1964, **86**, 5140–5144.
- 51 H. R. Allcock, *Acc. Chem. Res.*, 1978, **11**, 81–87.
- 52 Y. Sakata, S. Furukawa, M. Kondo, K. Hirai, N. Horike, Y. Takashima, H. Uehara, N. Louvain, M. Meilikhov, T. Tsuruoka, S. Isoda, W. Kosaka, O. Sakata and S. Kitagawa, *Science*, 2013, **339**, 193–196.
- 53 T. Tozawa, J. T. Jones, S. I. Swamy, S. Jiang, D. J. Adams, S. Shakespeare, R. Clowes, D. Bradshaw, T. Hasell, S. Y. Chong, C. Tang, S. Thompson, J. Parker, A. Trewin, J. Bacsá, A. M. Slawin, A. Steiner and A. I. Cooper, *Nat. Mater.*, 2009, **8**, 973–978.
- 54 J. T. Jones, T. Hasell, X. Wu, J. Bacsá, K. E. Jelfs, M. Schmidtman, S. Y. Chong, D. J. Adams, A. Trewin, F. Schiffman, F. Cora, B. Slater, A. Steiner, G. M. Day and A. I. Cooper, *Nat. Mater.*, 2011, **10**, 367–371.
- 55 L. Chen, P. S. Reiss, S. Y. Chong, D. Holden, K. E. Jelfs, T. Hasell, M. A. Little, A. Kewley, M. E. Briggs, A. Stephenson, K. M. Thomas, J. A. Armstrong, J. Bell, J. Busto, R. Noel, J. Liu, D. M. Strachan, P. K. Thallapally and A. I. Cooper, *Nat. Mater.*, 2014, **13**, 954–960.
- 56 M. Liu, L. Zhang, M. A. Little, V. Kapil, M. Ceriotti, S. Yang, L. Ding, D. L. Holden, R. Balderas-Xicohtencatl, D. He, R. Clowes, S. Y. Chong, G. Schutz, L. Chen, M. Hirscher and A. I. Cooper, *Science*, 2019, **366**, 613–620.
- 57 K. E. Jelfs, X. Wu, M. Schmidtman, J. T. Jones, J. E. Warren, D. J. Adams and A. I. Cooper, *Angew. Chem., Int. Ed.*, 2011, **50**, 10653–10656.
- 58 N. Giri, M. G. Del Popolo, G. Melaugh, R. L. Greenaway, K. Ratzke, T. Koschine, L. Pison, M. F. Gomes, A. I. Cooper and S. L. James, *Nature*, 2015, **527**, 216–220.
- 59 J. Tian, P. Thallapally, J. Liu, G. J. Exarhos and J. L. Atwood, *Chem. Commun.*, 2011, **47**, 701–703.
- 60 P. K. Thallapally, B. P. McGrail, S. J. Dalgarno, H. T. Schaefer, J. Tian and J. L. Atwood, *Nat. Mater.*, 2008, **7**, 146–150.
- 61 P. K. Thallapally, L. Dobrzanska, T. R. Gingrich, T. B. Wirsig, L. J. Barbour and J. L. Atwood, *Angew. Chem., Int. Ed.*, 2006, **45**, 6506–6509.
- 62 J. L. Atwood, L. J. Barbour, A. Jerga and B. L. Schottel, *Science*, 2002, **298**, 1000–1002.
- 63 R. W. Fessenden and P. Neta, *Chem. Phys. Lett.*, 1973, **18**, 14–17.
- 64 C. Reichardt, *Chem. Rev.*, 1994, **94**, 2319–2358.